

Silicon carbide microdisk resonator

Xiyuan Lu,¹ Jonathan Y. Lee,² Philip X.-L. Feng,³ and Qiang Lin^{2,4,*}

¹Department of Physics and Astronomy, University of Rochester, Rochester, New York 14627, USA

²Department of Electrical and Computer Engineering, University of Rochester, Rochester, New York 14627, USA

³Department of Electrical Engineering and Computer Science, Case Western Reserve University, Cleveland, Ohio 44106, USA

⁴Institute of Optics, University of Rochester, Rochester, New York 14627, USA

*Corresponding author: qiang.lin@rochester.edu

Received February 20, 2013; revised March 11, 2013; accepted March 12, 2013;
posted March 12, 2013 (Doc. ID 185514); published April 10, 2013

We demonstrate a silicon carbide (SiC) microdisk resonator with an intrinsic optical quality factor of 6.19×10^3 , fabricated on the 3C-SiC-on-Si platform. We characterize the temperature dependence of the cavity resonance and obtain a thermo-optic coefficient of $2.92 \times 10^{-5}/\text{K}$ for 3C-SiC. Our simulations show that the device exhibits great potential for cavity optomechanical applications. © 2013 Optical Society of America

OCIS codes: 230.5750, 130.3120, 220.4000, 160.3130.

High- Q optical microresonators are able to dramatically enhance optical fields inside a small volume, which is essential for a variety of applications including nonlinear optics [1], quantum optics [2], and cavity optomechanics [3]. In general, the underlying materials play a crucial role since most applications rely on the linear/nonlinear optical property [1], the mechanical property [3], the quantum confinement effect [4], or defect characteristics [5]. In recent years, significant interest has been focused on developing microresonators on various material platforms, including dielectrics [1,6–11], semiconductors [12–14], and polymers [15]. However, high- Q microresonators generally exhibit large thermal and mechanical sensitivities, making them challenging for practical application. Some materials, such as silicon and gallium arsenide, have small bandgaps that limit the operating spectral range. Others, such as lithium niobate and chalcogenide glass, exhibit the photorefractive effect or two-photon absorption, making it challenging to handle high optical powers. For micro/nanophotonic applications, it is crucial to search for a material platform with combined superior optical, mechanical, and thermal properties.

Silicon carbide (SiC) exhibits very attractive material characteristics [16]. It has a wide bandgap >2.3 eV with a transparent window covering from visible to midinfrared. It has a large refractive index of ~ 2.6 , which enables strong confinement of optical modes. In particular, it exhibits a significant thermal conductivity of 320–490 W/(mK), about 1–2 orders of magnitude larger than most other materials, thus enabling excellent heat management, which is particularly suitable for handling high optical powers. Moreover, SiC has a hardness and chemical inertness much greater than conventional optical materials, thus making it resistant to harsh environment. Therefore, SiC is an excellent material for photonic application.

SiC is a semiconducting polymorphic material that exists in various crystal structures [16]. One of its crystalline forms, 6H-SiC, was recently used to make photonic crystals [17]. However, 6H-SiC exhibits strong optical anisotropy due to its hexagonal wurtzite-like crystal structure. For photonic applications, an isotropic optical property is more favorable as it much more easily manages optical polarization. Among various SiC crystal

polytypes, 3C-SiC exhibits isotropic optical properties because of its zinc-blende crystal structure. Moreover, 3C-SiC is the only material form of SiC that currently can be grown directly on a silicon substrate by heteroepitaxy, thus with great potential for future optoelectronic integration. In this Letter, we demonstrate the first optical microresonator based upon 3C-SiC.

The single-crystalline 3C-SiC was epitaxially grown on a (100) silicon substrate by the two-step atmospheric-pressure chemical vapor deposition [18,19], with surface roughness optimized to minimal levels (~ 0.5 – 1 nm). A disk geometry was patterned by electron-beam lithography and etched by reactive ion etching with CF_4/Ar plasma, optimized to form the well-defined device structure. The silicon substrate was undercut by XeF_2 to form the supporting pedestal. Figure 1 shows the scanning electron microscopic image of the device with a radius of $15 \mu\text{m}$ and a thickness of 200 nm.

A continuous-wave tunable laser was launched into the whispering gallery microdisk resonator by near-field evanescent coupling through a tapered optical fiber, which also delivered the transmitted wave out of the device (Fig. 2). The cavity transmission spectrum was obtained by scanning the laser wavelength and recording the cavity transmission accordingly.

Figure 3 shows the laser-scanned cavity transmission for a quasi-transverse-electric-like (quasi-TE-like) cavity mode with polarization lying in the disk plane. Fitting the

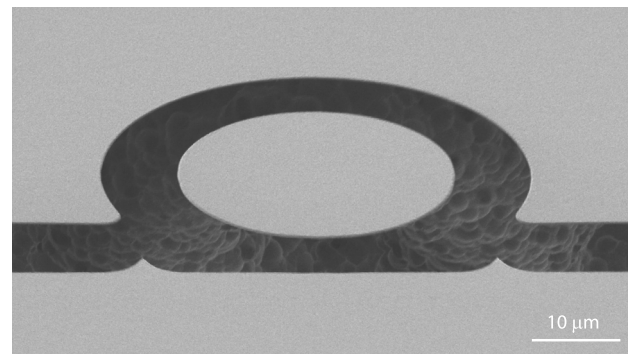


Fig. 1. Scanning electron microscopic image of an SiC microdisk resonator with a radius of $15 \mu\text{m}$ and a thickness of 200 nm, sitting on a silicon pedestal.

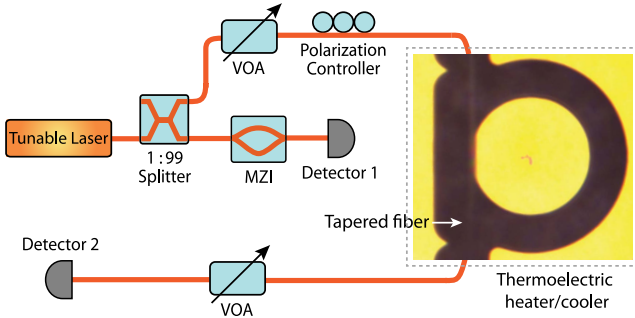


Fig. 2. (Color online) Schematic of the experimental setup for testing the SiC microdisk. VOA, variable optical attenuator; MZI, Mach-Zehnder interferometer. The device temperature is adjusted by a thermoelectric heater/cooler.

cavity spectrum, we obtain an intrinsic optical Q factor of 6.19×10^3 . Similar optical Q factors were observed on cavity resonant modes with different radial orders. The magnitude of optical Q in the current device is primarily limited by the sidewall roughness of the microdisk, not by diffraction-induced radiation [simulations by the finite-element method (FEM) indicate a radiation-limited optical Q of $\sim 10^{16}$]. Therefore, we expect the optical Q can be significantly improved with further optimization of the fabrication procedure (e.g., the plasma flow rates and the etching powers).

To investigate the thermo-optic property of the device, we changed the device temperature T by ~ 50 deg and recorded the cavity resonance tuning. Figure 4 shows that the cavity resonance changes linearly with the device temperature. As the cavity resonance wavelength λ is determined by the effective modal index n and mode radius R as $2\pi nR = m\lambda$, where m is the mode number, the temperature dependence is given by

$$\frac{1}{n} \frac{dn}{dT} = \frac{1}{\lambda} \frac{d\lambda}{dT} - \frac{1}{R} \frac{dR}{dT}. \quad (1)$$

For an SiC microdisk with a radius of $15 \mu\text{m}$, FEM simulations show that the mode radius scales linearly

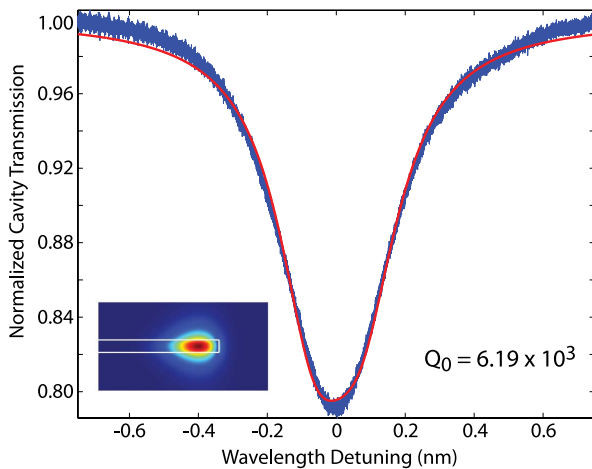


Fig. 3. (Color online) Normalized transmission for a quasi-TE-like cavity mode located at 1553.1 nm , with a theoretical fitting on top of the experimental trace. The inset shows the simulated optical field profile.

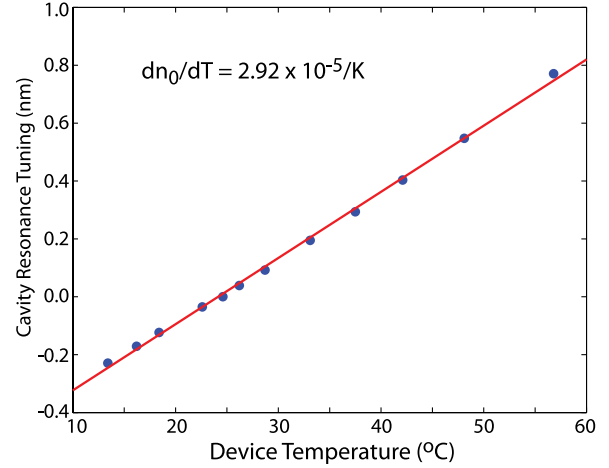


Fig. 4. (Color online) Tuning of cavity resonance as a function of device temperature, with experimental data shown in dots and linear fitting in solid line. The red curve shows a linear fitting.

with the physical radius of the microdisk. As a result, the temperature dependence of the mode radius is determined by the linear thermal expansion coefficient of 3C-SiC, with a value of $(1/R)(dR/dT) = 3.26 \times 10^{-6}/\text{K}$ at room temperature [20]. On the other hand, the optical mode is strongly confined inside the device (inset of Fig. 3, with an energy confinement factor of 92%). As a result, the temperature dependence of n is primarily determined by the thermo-optic coefficient of 3C-SiC material, $(1/n_0)(dn_0/dT) = (1/n)(dn/dT)$, where n_0 is the refractive index of 3C-SiC material. Using this expression together with Eq. (1) and fitting Fig. 4 with a linear curve, we obtain the thermo-optic coefficient of $(dn_0/dT) = 2.92 \times 10^{-5}/\text{K}$ at room temperature. This value is about 14% smaller than that measured from polycrystalline 3C-SiC [21] possibly due to the single-crystalline nature of our device material. It is about 25% smaller than that recently obtained from 6H-SiC photonic crystals [22], indicating the better thermal-optical stability of 3C-SiC devices. Moreover, it is about 5–10 times smaller than those of silicon and gallium arsenide and only nearly three times larger than that of silica [23], thus showing the great thermal-optical property of 3C-SiC.

A SiC microdisk resonator exhibits great potential for many applications. One example is to take advantage of the superior mechanical property of 3C-SiC, which exhibits a Young's modulus of $\sim 450 \text{ GPa}$ [16], significantly larger than other materials used for mesoscopic mechanical structures [3,24]. It is thus particularly useful for making high-frequency optomechanical oscillators, which are essential for frequency metrology and time keeping [24]. Figure 5 compares the frequencies of the fundamental radial-stretching mechanical mode (Fig. 5, inset), in microdisks made with different materials. It shows clearly that 3C-SiC microdisks offer mechanical frequencies about 30%–170% larger than silicon nitride, silicon, silica, and gallium arsenide devices. SiC devices are expected to have a high mechanical Q , as indicated by recent SiC-based nanoelectromechanical devices [25].

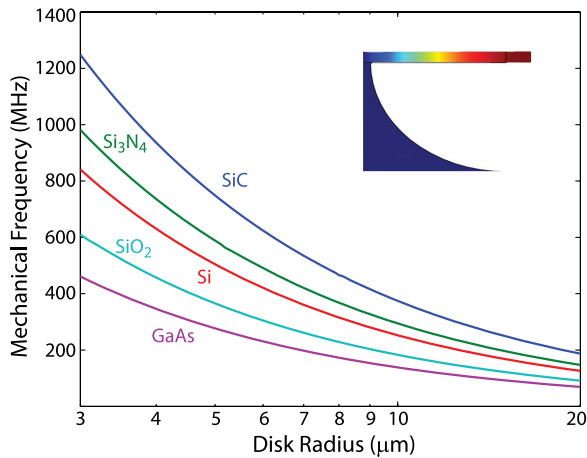


Fig. 5. (Color online) FEM-simulated mechanical frequency for the fundamental radial-stretching mode in a 200 nm thick microdisk. The inset shows the mechanical mode profile.

The optomechanical coupling in a microdisk resonator is given by $g_{om} = -(\omega_0/R)$, where ω_0 is the cavity resonance frequency. A microdisk with a radius of 10–20 μm results in $(|g_{om}|/2\pi) = 10\text{--}20$ GHz/nm for a telecom-band wavelength. In particular, FEM simulations show that 3C-SiC allows us to well confine optical modes inside a microdisk with a radius of only 2.5 μm and a thickness of 400 nm, which is not possible for a silica or silicon nitride microdisk. Such a device exhibits a strong $|g_{om}|/2\pi$ of 80 GHz/nm and a mechanical frequency of 1.5 GHz. The optomechanical coupling will be further doubled for cavity modes at near infrared around 700–800 nm, which is inaccessible for silicon and gallium arsenide devices due to the material absorption. Therefore, 3C-SiC microdisk exhibits great potential for cavity-optomechanical application.

In conclusion, we have demonstrated, for the first time to the best of our knowledge, a 3C-SiC microdisk resonator. The device exhibits an intrinsic optical Q of 6.19×10^3 . Detailed characterization shows a thermo-optic coefficient of $2.92 \times 10^{-5}/\text{K}$ for 3C-SiC at room temperature, indicating the great thermal-optical property of 3C-SiC devices. Our numerical simulations show that the device is well suited for applications in cavity optomechanics. Further optimization of the fabrication procedure will significantly improve the optical Q .

This work was supported by the Air Force Office of Scientific Research under grant no. FA9550-12-1-0419. It was performed in part at the Cornell NanoScale Facility, a member of the National Nanotechnology

Infrastructure Network, which is supported by the National Science Foundation (grant ECS-0335765). P. X. L. Feng thanks support from the Case School of Engineering.

References

1. K. J. Vahala, *Nature* **424**, 839 (2003).
2. H. J. Kimble, *Phys. Scr.* **T76**, 127 (1998).
3. T. J. Kippenberg and K. J. Vahala, *Science* **321**, 1172 (2008).
4. S. Noda, M. Fujita, and T. Asano, *Nat. Photonics* **1**, 449 (2007).
5. A. Faraon, P. E. Barclay, C. Santori, K.-M. C. Fu, and R. G. Beausoleil, *Nat. Photonics* **5**, 301 (2011).
6. J. Hu, N. Carlie, L. Petit, A. Agarwal, K. Richardson, and L. Kimerling, *Opt. Lett.* **33**, 761 (2008).
7. W. Liang, A. A. Savchenkov, A. B. Matsko, V. S. Ilchenko, D. Seidel, and L. Maleki, *Opt. Lett.* **36**, 2290 (2011).
8. Y. Okawachi, K. Saha, J. S. Levy, Y. H. Wen, M. Lipson, and A. L. Gaeta, *Opt. Lett.* **36**, 3398 (2011).
9. M. Mohageg, A. B. Matsko, and L. Maleki, *Opt. Express* **20**, 16704 (2012).
10. T.-J. Wang, J.-Y. He, C.-A. Lee, and H. Niu, *Opt. Express* **20**, 28119 (2012).
11. C. Xiong, K. Sun, K. Y. Fong, and H. X. Tang, *Appl. Phys. Lett.* **100**, 171111 (2012).
12. M. Borselli, T. J. Johnson, and O. Painter, *Opt. Express* **13**, 1515 (2005).
13. L. Ding, C. Baker, P. Senellart, A. Lemaitre, S. Ducci, G. Leo, and I. Favero, *Phys. Rev. Lett.* **105**, 263903 (2010).
14. J. T. Choy, J. D. B. Bradley, P. B. Deotare, I. B. Burgess, C. C. Evans, E. Mazur, and M. Lončar, *Opt. Lett.* **37**, 539 (2012).
15. T. Grossmann, M. Hauser, T. Beck, C. Gohn-Kreuz, M. Karl, H. Kalt, C. Vannahme, and T. Mappes, *Appl. Phys. Lett.* **96**, 013303 (2010).
16. G. L. Harris, ed., *Properties of Silicon Carbide* (IEE INSPEC, 1995).
17. B.-S. Song, S. Yamada, T. Asano, and S. Noda, *Opt. Express* **19**, 11084 (2011).
18. S. Nishino, J. A. Powell, and H. Will, *Appl. Phys. Lett.* **42**, 460 (1983).
19. C. A. Zorman, A. J. Fleischman, A. S. Dewa, M. Mehregany, C. Jacob, S. Nishino, and P. Pirouz, *J. Appl. Phys.* **78**, 5136 (1995).
20. Z. Li and R. C. Bradt, *J. Am. Ceram. Soc.* **70**, 445 (1987).
21. W. J. Tropf and M. E. Thomas, *Johns Hopkins APL Technical Digest* **19**, 293 (1998).
22. S. Yamada, B.-S. Song, T. Asano, and S. Noda, *Opt. Lett.* **36**, 3981 (2011).
23. M. Bass, G. Li, and E. Van Stryland, eds., *Handbook of Optics*, 3rd ed., Vol. **IV** (Optical Society of America, 2010).
24. C. T.-C. Nguyen, *IEEE Trans. Ultrason. Ferroelectr. Freq. Control* **54**, 251 (2007).
25. V. Cimalla, J. Pezoldt, and O. Ambacher, *J. Phys. D* **40**, 6386 (2007).